Transport Effects and Characteristic Modes in the Modeling and Simulation of Submicron Devices

Joseph W. Jerome*and Chi-Wang Shu†

Revised September, 1994

Abstract

This paper has two major goals: (1) to study the effect of the common practice of neglecting the convective terms (inertial approximation) in the hydrodynamic model in the simulation of n^+-n-n^+ diodes and two dimensional MESFET devices; and, (2) to test analytical criteria, formulated in terms of characteristic values of the Jacobian matrix, as a method of determining the impact of first derivative perturbation terms in this model, and in related energy transport models. This characteristic value analysis can be thought of as generalizing the usual analytical solution of first order linear systems of ordinary differential equations with constant coefficients. Concerning (1), we find that the inertial approximation is invalid near the diode junctions, and near the contact regions of the MESFET device. In regard to (2), we find a proper arrangement of terms, expressing the flux, such that the first derivative part of the system is hyperbolic, both for the hydrodynamic model and the energy transport model. For the hydrodynamic model, two forms of the heat conduction term are studied, including the case of a convective term. This suggests and validates the use of shock capturing algorithms for the simulation.

*Department of Mathematics, Northwestern University, Evanston, IL 60208
†Division of Applied Mathematics, Brown University, Providence, RI 02912

1 Introduction

In earlier work (see [8]), we have advocated using modern nonlinear hyperbolic based shock capturing algorithms (e.g., the ENO algorithm in [16]) in device simulations with hydrodynamic (HD) and energy transport (ET) models; introductions to these models may be found in [13] and [2], respectively. The first use of such methods in device simulation was [3]. They are very successful in solving a hyperbolic conservation law of the form:

$$w_t + f_1(w)_x + f_2(w)_y = 0, \tag{1.1}$$

where w is a vector. In device simulation, both HD and ET models can be expressed in the following form:

$$w_t + f_1(w)_x + f_2(w)_y = r(w), \tag{1.2}$$

where the right-hand-side $r(w)$ contains both the forcing terms due to the relaxation, which are nonlinear functions of w, and the second derivative terms due to the heat conduction. A necessary precondition for the usage of hyperbolic based shock capturing algorithms is the property that the first derivative part, $f_1(w)_x + f_2(w)_y$, is indeed hyperbolic, i.e., $\xi_1 f_1'(w) + \xi_2 f_2'(w)$, with real ξ_1 and ξ_2, has only real eigenvalues and a complete set of eigenvectors. Here, f_i' denotes the Jacobian, $\partial f_i / \partial w$, for $i = 1, 2$. A common practice in the interpretation of the hydrodynamic model is to employ the inertial approximation, which in our terminology characterizes the transport effect as small if

$$\tau_p \sqrt{u_x^2 + u_y^2 + v_x^2 + v_y^2} \ll 1, \tag{1.3}$$

where τ_p is the momentum relaxation coefficient and (u, v) is the velocity vector. Here we use u_x to denote the partial derivative of u with respect to x, i.e. $\partial u / \partial x$, etc. Note that the velocity derivatives, rather than the velocities themselves, appear in (1.3). The corresponding one dimensional version is similar. The reader can find this approximation employed in many

2

reduced hydrodynamic models (cf. [11]), where it is typically accompanied by the assumption that the kinetic energy component is negligible in the total energy. As discussed in [13], the use of (1.3) allows the extension of the Scharfetter-Gummel method to a hydrodynamic model setting. A comparable hypothesis is well known in fluid mechanics, where the resulting flow is termed a Stokes' flow. In the electrical engineering community, one speaks of neglecting the convective terms.

In this paper, we simulate a standard one dimensional n^+-n-n^+ channel and a two dimensional MESFET, using the complete HD model, as introduced in [13], with Baccarani-Wordeman relaxation expressions (see [1]), and then check the validity of (1.3). From a physical point of view, we wish to check whether the transport effect is uniformly small. If it is, hyperbolic based algorithms probably need not be used, and the inertial approximation would appear justified. We can see from the simulations in the sequel (cf. §2) that the quantity measured by the left-hand-side of (1.3) is not small near the junctions for the one dimensional case, and near the contact regions for the two dimensional case. This verifies that the transport effect is not uniformly small, and justifies the usage of hyperbolic based algorithms, at least in the cases where computational resources limit the number of grid points one can put inside the junction regions to fully resolve them. It also justifies using the full hydrodynamic model. We are not aware of any prior work which tests the validity of (1.3) intrinsically, i.e., by using the hydrodynamic model itself. Notice that this is logically different from an extrinsic check via, say, the Boltzmann transport equation as employed in [17] to measure the effect on the kinetic energy calculation near the diode junctions. Moreover, the kinetic energy component is distinct from the calculation of the left-hand-side of (1.3).

The reader will notice that hyperbolicity means, via a separation of variables analysis involving imaginary exponentials, that an oscillatory dependence on the spatial variables results in a time dependence which neither grows nor decays. This results from separated solutions of

the linearized problem of the form,

$$w = w_0 \exp(i(\xi_1 x + \xi_2 y)) \exp(i\lambda t). \tag{1.4}$$

Our assumption requires λ to be real. Notice that if this is not true, the system is of mixed hyperbolic-elliptic type, and the mathematical theory about the solution to (1.2), when the right-hand-side tends to zero, is very complicated and in many cases still unresolved. Likewise, numerical methods for such mixed type systems are also complicated and not fully developed (see e.g., [15]). We would thus desire to avoid the appearance of mixed type first derivative part when modifying the models. Notice also that in many modifications to the hydrodynamic models (e.g., [17], [12]), the right-hand-side of (1.2) is changed to contain some first derivative terms also. Although in practical computations these terms are treated as small perturbations and approximated separately, the justification that these terms are indeed "small" can only come from moving these terms to the left-hand-side, absorbing them into $f_1(w)$ and $f_2(w)$, and then checking hyperbolicity. We discuss such a hyperbolicity check for the standard HD model, the modified HD model [17], and the ET model [2]. Another aspect of hyperbolicity comes from a comparison of the hyperbolic part with the heat conduction term in the energy equation; this comparison may be characterized by the stability condition, which is imposed on the explicit numerical scheme. This paper does not address the latter issue directly, but we experience no undue time step restrictions, induced by high density doping, relaxation, etc., with the numerical scheme.

The numerical scheme we use in this paper is the ENO (Essentially Non-Oscillatory) scheme [16], adapted to device simulations in [3] and [8]. It has the advantage of both high order accuracy and monotone sharp gradient transitions.

2 The Transport Effect

Both the HD (hydrodynamic) and ET (energy transport) models can be written in a conservation law format with other terms lumped into the right-hand-side, given by (1.2). The transport effect can be expressed by the quantity $\tau_p |u_x|$ in one space dimension, and by $\tau_p \sqrt{u_x^2 + u_y^2 + v_x^2 + v_y^2}$ in two space dimensions, where τ_p is the momentum relaxation coefficient, and u or (u, v) is the velocity. Again, we note that u_x denotes the derivative of the velocity, $u_x = \partial u / \partial x$. A common practice in device modeling is to employ the inertial approximation, which requires that the transport effect is uniformly small:

$$|u \cdot \nabla u| \ll \frac{|u|}{\tau_p}, \tag{2.1}$$

which is implied by

$$\tau_p |u_x| \ll 1, \tag{2.2}$$

in one space dimension, and

$$\tau_p \sqrt{u_x^2 + u_y^2 + v_x^2 + v_y^2} \ll 1, \tag{2.3}$$

in two space dimensions. In order to verify whether these commonly assumed properties are valid, we simulate, using the full HD model [13], both a one dimensional n^+-n-n^+ channel, and a two dimensional MESFET. We note in passing that the Stokes' flow assumption in fluid mechanics assumes the left hand side of (2.1) is small in relation to the pressure gradient/density ratio in steady-state.

The one dimensional n^+-n-n^+ channel we simulate is a standard silicon diode with a length of $0.6\mu m$, with a doping defined by $n_d = 5 \times 10^{17} cm^{-3}$ in $[0, 0.1]$ and in $[0.5, 0.6]$, and $n_d = 2 \times 10^{15} cm^{-3}$ in $[0.15, 0.45]$, joined by smooth junctions (Fig. 1). The lattice temperature is taken as $T_0 = 300$ K. We apply a voltage bias of $vbias = 0.5$V, 1.0V and 1.5V, respectively. We use the full HD model; the relevant parameters can be found in [8]. We use a high order ENO

scheme (third order) and a very refined grid (200 points), in order to ensure that the physical model is fully resolved by our numerical result.
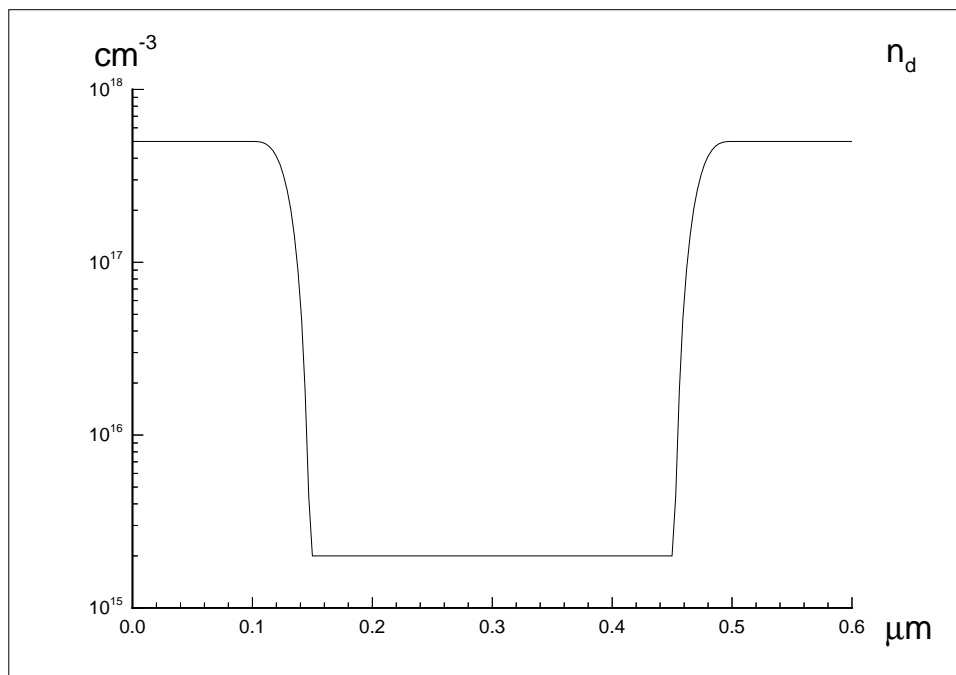
Fig. 1: The one dimensional n^+-n-n^+ channel: the doping n_d in the logarithm scale.

From the computed velocity, we can easily obtain the transport effect $\tau_p|u_x|$. This should be uniformly small as described in (2.2), in order to justify the assumption of the inertial approximation. However, our result in Fig. 2 clearly shows that the transport effect is *not* small near the junctions. The velocity itself, for the case $vbias = 1.5$V, is shown in Fig. 3.

Fig. 2: The one dimensional n^+-n-n^+ channel: the transport effect $\tau_p u_x$ using the HD model.

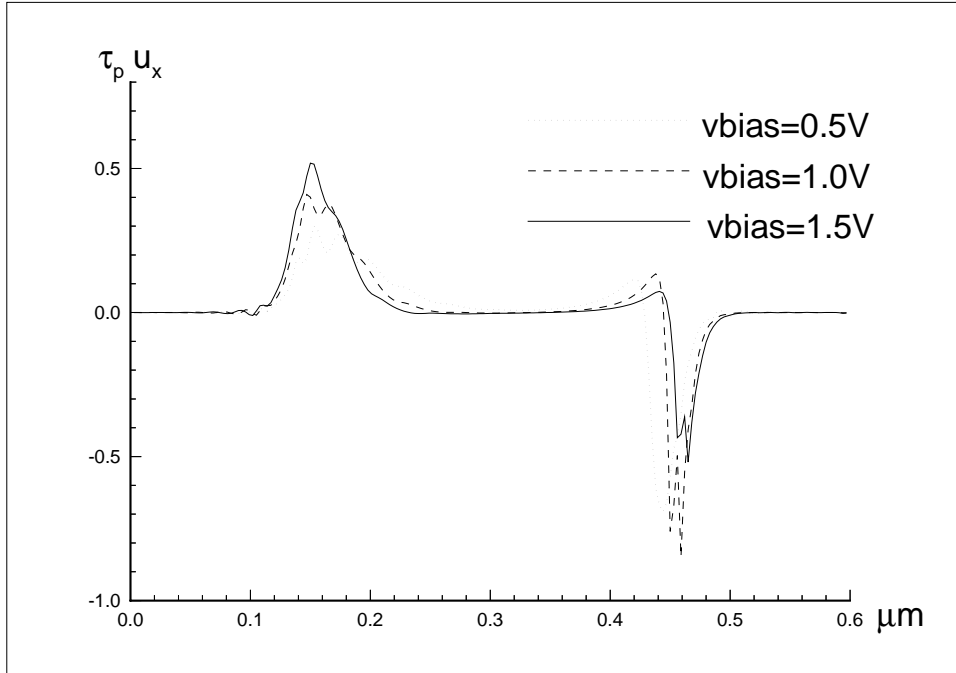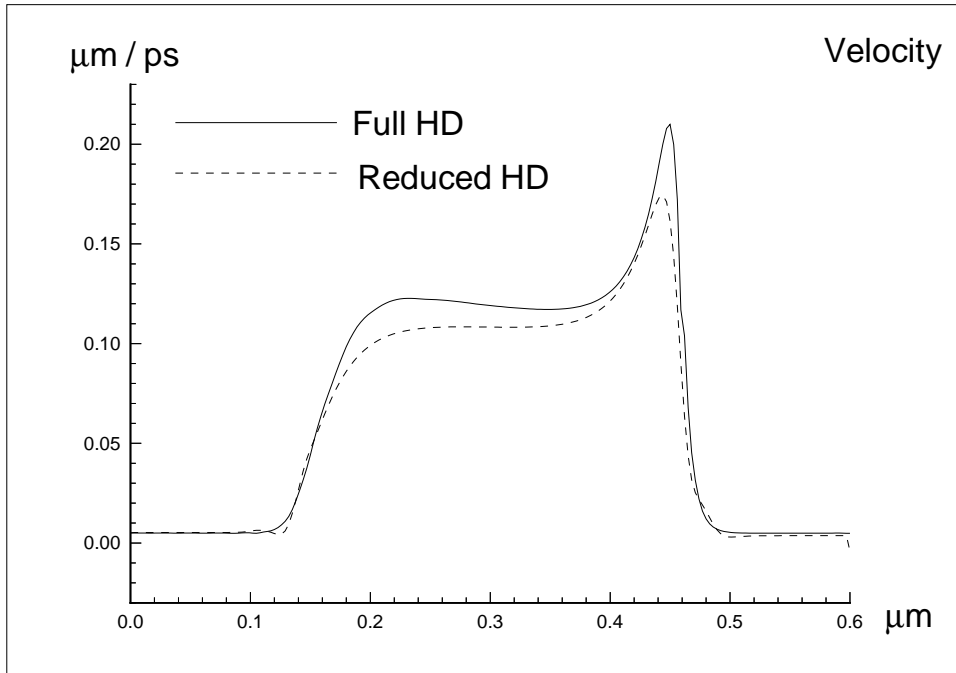Fig. 3: The one dimensional n^+-n-n^+ channel: the velocity u using the HD model and the reduced HD model with the inertial assumption.

In order to verify that this is not an artifact of the spurious velocity overshoot at the right

junction, we also simulate with a reduced heat conduction coefficient $\kappa_0 = 0.5$ to reduce this spurious overshoot (see [7]). The result, Fig. 4, still shows a significant transport effect at the junctions, especially at the left junction, although the spurious velocity overshoot is greatly reduced (Fig. 5).
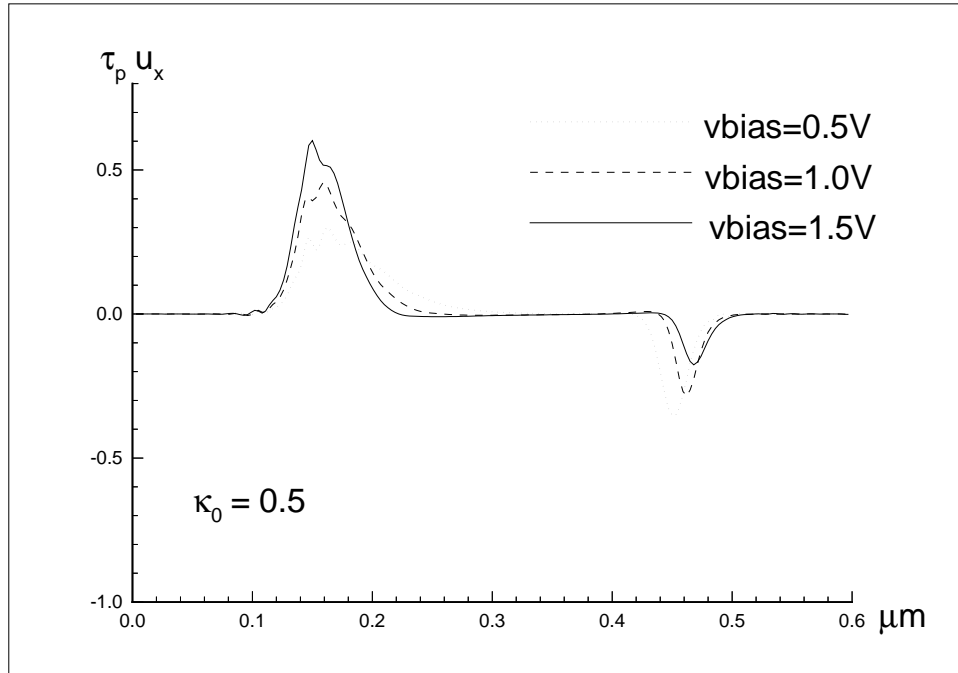
Fig. 4: The one dimensional n^+-n-n^+ channel: the transport effect $\tau_p u_x$ using the HD model with a reduced heat conduction $\kappa_0 = 0.5$.
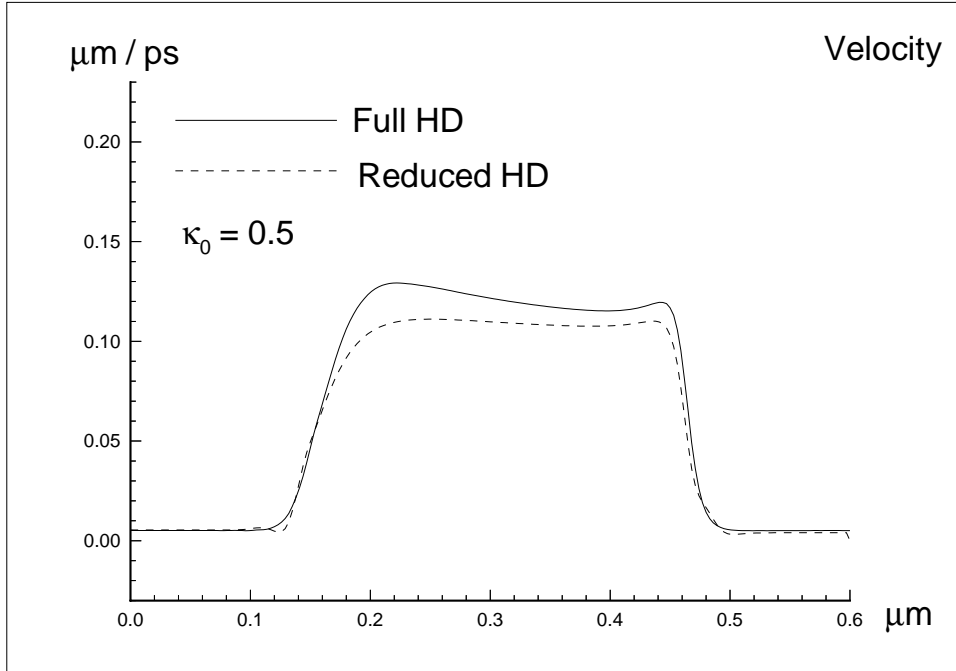
Fig. 5: The one dimensional n^+-n-n^+ channel: the velocity u using the HD model with a reduced heat conduction $\kappa_0 = 0.5$, and the reduced HD model with the inertial assumption using the same reduced heat conduction.

Another concern about the definition of the transport effect (2.2), is that it depends on the relaxation coefficient τ_p, which is subject to modeling errors, especially near the junctions. To reduce this artifact, we also simulate the same device with a doping dependent mobility coefficient μ_0 (see [9]). We can see that the transport effect remains large at the junctions, especially at the left junction, in Fig. 6, although the spurious velocity overshoot is greatly reduced (Fig. 7). Notice that this reduction occurs even with $\kappa_0 = 1.5$.

Fig. 6: The one dimensional n^+-n-n^+ channel: the transport effect $\tau_p u_x$ using the HD model with a doping dependent variable mobility μ_0.
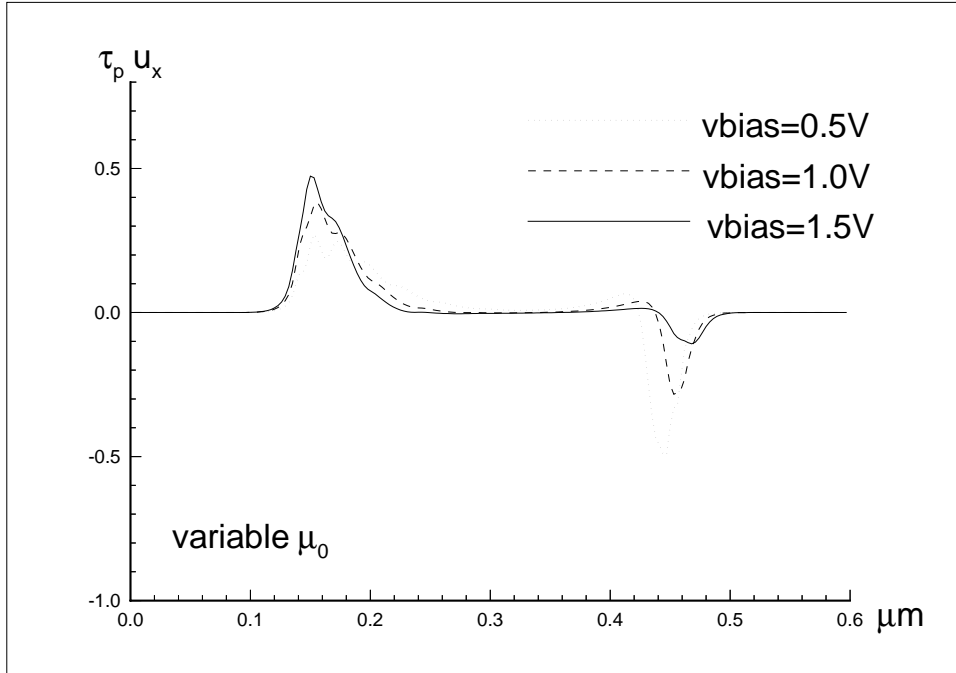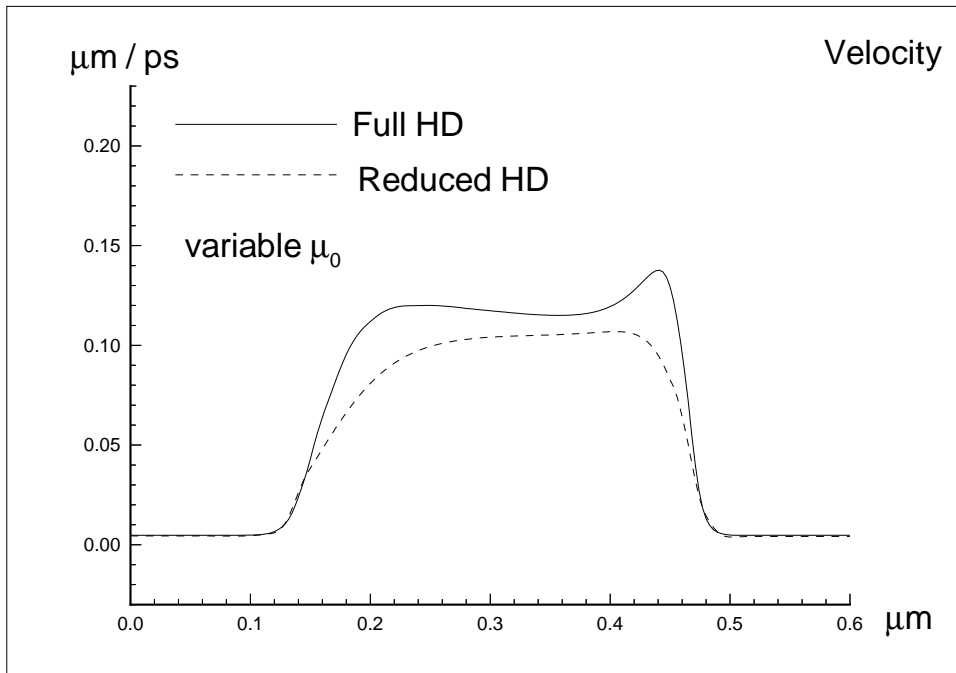

Fig. 7: The one dimensional n^+-n-n^+ channel: the velocity u using the HD model with a doping dependent variable mobility μ_0, and the reduced HD model with the inertial assumption using the same variable mobility.

To determine the effect of ignoring this transport effect, by using a reduced hydrodynamic model, we also carry out the simulation of the same diode using the reduced HD model, with the inertial assumptions (i.e., the assumption that $\tau_p u_x = 0$ and the assumption that the kinetic energy is negligible in the total energy). This reduced HD model does not have a momentum equation, is a fully parabolic system, hence is much easier to solve numerically. The velocity is a quantity derived from the concentration and energy. As a matter of fact, for this simplified HD model, a simple central difference approximation can be used when the equivalent first order system is employed. We can see from Figs. 3, 5, and 7 that the reduced HD model underestimates the velocity in all the cases, throughout the middle region but especially near the left junction. This is similar to what would happen if one uses the drift diffusion model, although the discrepancy is less serious.

Next, we turn our attention to two space dimensions. We simulate a two dimensional MESFET of the size $0.6 \times 0.2 \mu m^2$. The source and the drain each occupies $0.1 \mu m$ at the upper left and the upper right, respectively, with a gate occupying $0.2 \mu m$ at the upper middle (Fig. 8). The doping is defined by $n_d = 3 \times 10^{17} cm^{-3}$ in $[0, 0.1] \times [0.15, 0.2]$ and in $[0.5, 0.6] \times [0.15, 0.2]$, and $n_d = 1 \times 10^{17} cm^{-3}$ elsewhere (also shown in Fig. 8). This is the example we used in [8]. We remark that in our numerical experiments, ENO schemes are stable and convergent for higher absolute dopings (experiments up to $10^{20} cm^{-3}$) and for higher doping ratios (experiments up to 10^5).
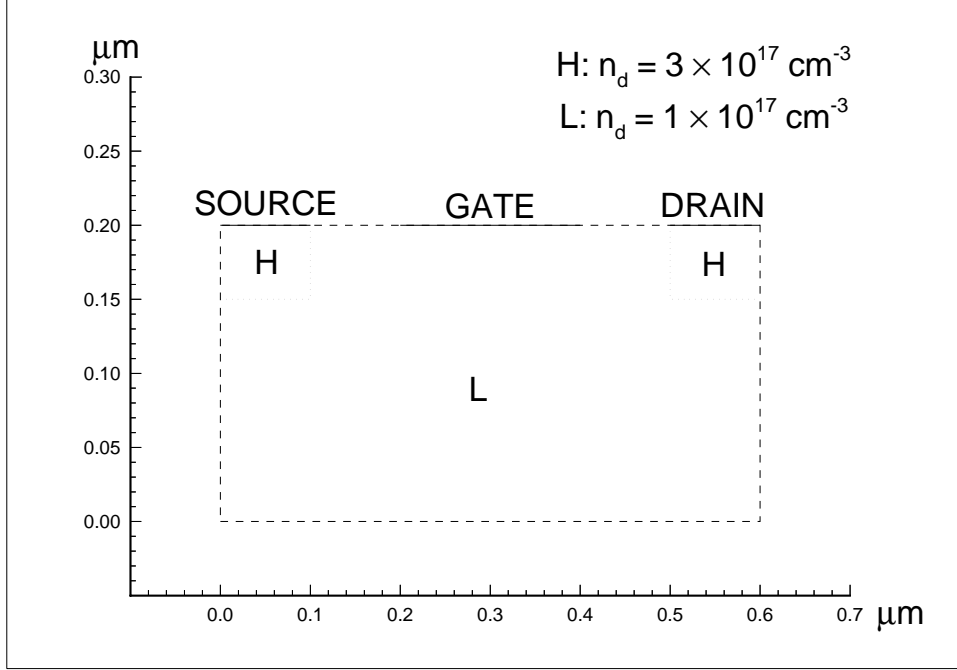
Fig. 8: The two dimensional MESFET: the geometry and the doping n_d.

We apply, at the drain, a voltage bias $vbias = 2$V. The gate is a Schottky contact, with a negative voltage bias $vgate = -0.8$V and a very low concentration value $n = 3.8503 \times 10^4 cm^{-3}$ (following Selberherr [14]). The lattice temperature is again taken as $T_0 = 300$ K. A high order (third order) ENO scheme with a very refined grid of 192×64 points is used. Again, this is to ensure that the physical model is fully resolved by the numerical scheme. We note that for this problem, the third order ENO scheme already gives very accurate results for a grid of the size 96×32 points. Boundary conditions and other parameters can be found in [8].

From the computed velocity, we obtain the transport effect $\tau_p \sqrt{u_x^2 + u_y^2 + v_x^2 + v_y^2}$. Again, this should be uniformly small as described in (2.3), in order to justify the neglect of the transport effect. However, our result in Fig. 9 shows that the transport effect is *not* small near the contacts. For easy presentation, we have listed an integer at every other grid point in the MESFET in Fig. 9. This integer is obtained by

$$\min \left(9, \ \left[10\tau_p \sqrt{u_x^2 + u_y^2 + v_x^2 + v_y^2} \right] \right),$$

12

where [a] denotes the greatest integer less than or equal to a. In other words, this integer is ten times the transport effect formula value, capped from above by nine. The velocity field itself is shown in Fig. 10.

```
0000000000000013585632333467999999999999999999999999999999999999985110000000112599999999999999998
0000000000000133454334456899999999875446422285434423433322333446721100000000113698877754322111000
0000000000001133223334445799999999996566555566444544444444444432100000000001123333322222211111
0000000000001122123334444579999999997875555455554444554444444433321100000000000011111111111000000
0000000000001121123344433444499799887565444444444443444443333222110000000000000000110000000000000
0000000000001122233333333333587787665444333333333333333333222211100000000000000000000000000000000
0000000000011111233333333222233566665444333332223333322222222211110000000000000000000000000000000
2222222222333333443333222222222334444433332222222222222222221111110000000000000000000000000000000
2222333333334444322222222222222333333222222222222222211111111111000000000000000000000000000000000
1111111122222322211111111122222222222222221111111111111111110000000000000000000000000000000000000
1111111111111111111111111111111111121111111111111111111111110000000000000000000000000000000000000
0000011111111111111111111111111111111111111111111111111111000000000000000000000000000000000000000
0000000111111111111111111111111111111111111111111110000000000000000000000000000000000000000000000
0000000001111111111111111111111111111111110000000000000000000000000000000000000000000000000000000
0000000111111111111111111111111111111111100000000000000000000000000000000000000000000000000000000
0000001111111111111111111111111111111111000000000000000000000000000000000000000000000000000000000
0111111111111111111111111111111111111110000000000000000000000000000000000000000000000000000000000
0111111111111111111111111111111111111110000000000000000000000000000000000000000000000000000000000
0111111111111111111111111111111111111100000000000000000000000000000000000000000000000000000000000
0111111111111111111111111111111111110000000000000000000000000000000000000000000000000000000000000
0111111111111111111111111111111111110000000000000000000000000000000000000000000000000000000000000
0000011111111111111111111111111111110000000000000000000000000000000000000000000000000000000000000
0100111111111111111111111111111110000000000000000000000000000000000000000000000000000000000000000
0100111111111111111111111111111110000000000000000000000000000000000000000000000000000000000000000
0111111111111111111111111111110000000000000000000000000000000000000000000000000000000000000000000
0111111111111111111111111111110000000000000000000000000000000000000000000000000000000000000001110
0111111111111111111111111111110000000000000000000000000000000000000000000000000000000000000011110
0111111111111111111111111111100000000000000000000000000000000000000000000000000000000000000011110
0111111111111111111111111111000000000000000000000000000000000000000000000000000000000000000111111
0111111111111111111111111111000000000000000000000000000000000000000000000000000000000000000111111
0111111111111111111111111111000000000000000000000000000000000000000000000000000000000000001111111
0111111111111111111110000000000000000000000000000000000000000000000000000000000000000000000000110
```
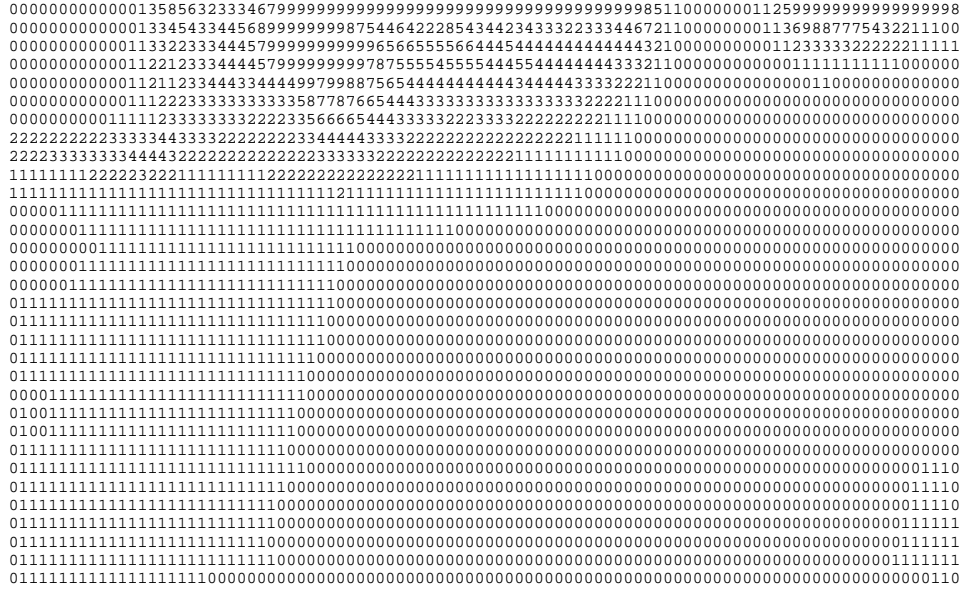
Fig. 9: The two dimensional MESFET: the transport effect. The integers denote the integer part of ten times the transport effect: $\left[10\tau_p \sqrt{u_x^2 + u_y^2 + v_x^2 + v_y^2} \right]$. If it is larger than 9, then 9 is shown.
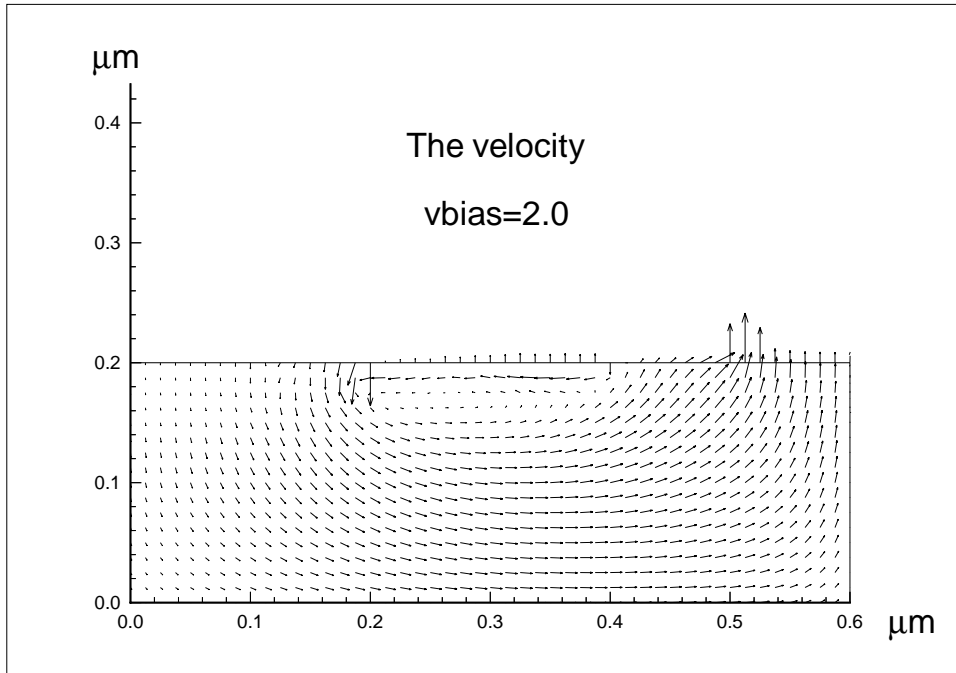
Fig. 10: The two dimensional MESFET: the velocity field (u, v).

From these two examples we can conclude that, in device simulations, the transport effect is not uniformly small. This justifies the usage of hyperbolic based shock capturing schemes (e.g., [16]) for device simulation. It also justifies the usage of the full HD model.

3 The Test for Hyperbolicity

In this section, we would like to check the hyperbolicity of the first derivative part in (1.2), for the HD model, the modified HD model in [17], and for the ET model in [2]. As indicated in the introduction, this check is necessary to justify the usage of hyperbolic based algorithms. It is also necessary to justify that any modifications to the physical model, such as the modification proposed in [17] to the HD model, indeed introduce only "small" perturbations to the original model. Here "small" means that the mathematical property of the underlying first order part of the partial differential equation is not fundamentally altered.

The first example to consider is the standard HD model, given by (1.2), with a left-hand-side

14

defined by

$$w = \begin{pmatrix} mn \\ mnu \\ mnv \\ E \end{pmatrix}, \qquad f(w) = \begin{pmatrix} mnu \\ mnu^2 + p \\ mnuv \\ u(E+p) \end{pmatrix}, \qquad g(w) = \begin{pmatrix} mnv \\ mnuv \\ mnv^2 + p \\ v(E+p) \end{pmatrix}, \qquad (3.1)$$

where n is the concentration, (u, v) is the velocity vector, E is the total energy per unit volume,

$p = (\gamma - 1)\left[E - \frac{1}{2}mn(u^2 + v^2)\right]$ is the pressure, with $\gamma = \frac{5}{3}$. We do not write out the right-

hand-side $r(w)$ (which includes the forcing terms due to the relaxation and the heat conduction

second derivative terms), since such terms do not affect our analysis.

Since (1.1), with the fluxes defined by (3.1), is just the Euler equation for a compressible gas,

it is well known that, for any real numbers ξ_1 and ξ_2, the linear combination of the Jacobians,

$\xi_1 f'(w) + \xi_2 g'(w)$, has only real eigenvalues $U - c, U, U, U + c$, where $U = \xi_1 u + \xi_2 v$ and $c = \sqrt{\frac{\gamma p}{mn}}$

is the sound speed. It also has two independent eigenvectors for the double eigenvalue U. The

HD model thus has a first derivative part (1.1) which is hyperbolic. Note that the sound speed

associated with the full system, not simply the first derivative part, is $c = \sqrt{\frac{p}{mn}}$. This fact

was discussed in [6] and [3], and emphasized in the derivation of classification described in [4]

and [5]. This has the implication that the sound speed experiences a discontinuity as the heat

conductivity tends to zero, reflective of the complex structure defined by the model.

Next, we consider the modification to the HD model suggested in [17]. Since only the

one dimensional case is considered there, we will also consider only the one dimensional case.

Although the modification can be formally considered as a presumably small perturbation, and

added to the right-hand-side of (1.2), a rigorous justification that it is indeed small can only

result from transferring the first derivative part of the modification to the left-hand-side, and

analyzing the hyperbolicity condition of the perturbed first derivative part. The new flux, as

was used in the numerical section of [17], can be written as

$$w = \begin{pmatrix} mn \\ mnu \\ E \end{pmatrix}, \qquad f(w) = \begin{pmatrix} mnu \\ mnu^2 + p \\ u(E+p) + \alpha mnu \end{pmatrix}, \qquad (3.2)$$

15

where again n is the concentration, u is the velocity, E is the total energy per unit volume, $p = (\gamma - 1)\left[E - \frac{1}{2}mnu^2\right]$ is the pressure, with $\gamma = \frac{5}{3}$. The perturbation coefficient α is expressed by

$$\alpha = -\frac{5}{2}(1 - r)\frac{kT_0}{m}, \tag{3.3}$$

with $r = 0.72$ (the choice suggested in [17] for computation), $k = 0.138046 \times 10^{-4}$, $T_0 = 300$, and $m = 0.26 \times 0.9109$ in our units. This results in a perturbation parameter,

$$\alpha = -0.0122404,$$

and we shall use this value to study the hyperbolicity of (3.2). Clearly,

$$f'(w) = \begin{pmatrix} 0 & 1 & 0 \\ \frac{\gamma-3}{2}u^2 & (3-\gamma)u & \gamma-1 \\ \frac{\gamma-2}{2}u^3 - \frac{uc^2}{\gamma-1} & \frac{3-2\gamma}{2}u^2 + \frac{c^2}{\gamma-1} + \alpha & \gamma u \end{pmatrix},$$

which differs from the Jacobian of the unperturbed case only slightly (the extra α at the third row, second column position). Notice that the Jacobian depends only upon the velocity u and the sound speed $c = \sqrt{\frac{\gamma p}{mn}}$. Unfortunately, this small difference produces a significant change in the analytic form of the eigenvalues of the Jacobian $f'(w)$. We thus resort to a numerical experiment, to determine whether the eigenvalues of $f'(w)$ are all real and distinct in the region of interest to us. To be more precise, we fill the region $0 \le u \le 0.3$ and $0.1 \le c \le 0.6$ (in the units of $\mu m/ps$) with a dense grid, then use a numerical eigenvalue routine to find the three eigenvalues of the Jacobian $f'(w)$ at each grid point. We then plot the region of non-hyperbolicity, that is, the region in which at least one of the eigenvalues of $f'(w)$ is not real (it happens that repeated eigenvalues did not appear). This region is shown as the dark region near the bottom in Fig. 11. We also plot the realized pairs (u, c) from the simulation of the one dimensional n^+-n-n^+ channel described before, for $vbias = 0.5V$, $1.0V$, and $1.5V$ respectively, in Fig. 11. We can clearly see that the modified system is hyperbolic for those realized (u, c) values. This verifies that the perturbation proposed in [17] does not change the hyperbolicity of the first derivative part for this n^+-n-n^+ channel.
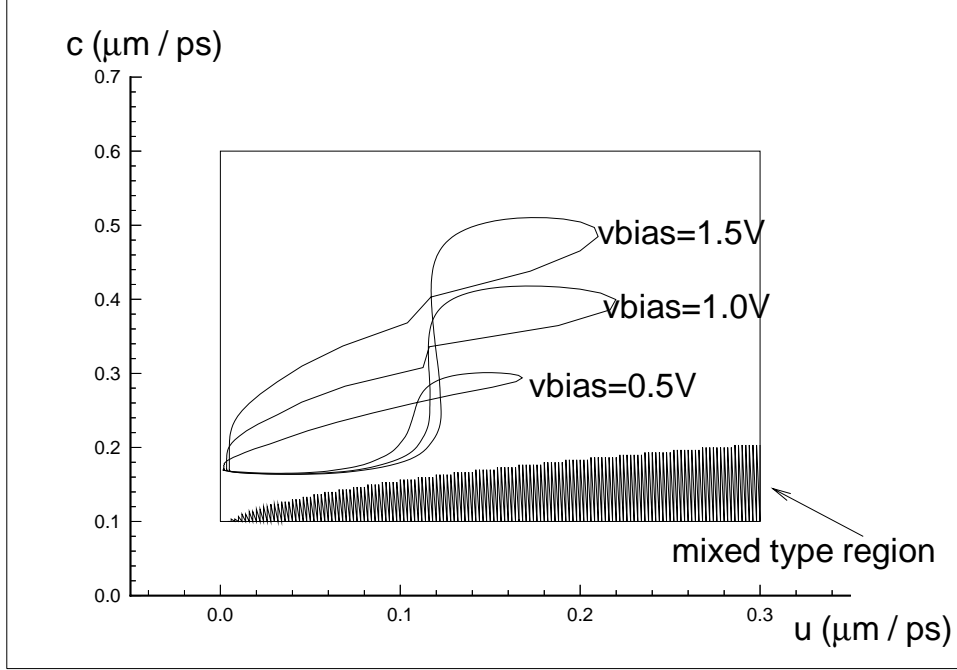
Fig. 11: The hyperbolicity check for (3.2)-(3.3). The dark region at the bottom is the region of non-hyperbolicity. The three closed loops are realized values of (u, c) for the one dimensional n^+-n-n^+ channel with $vbias = 0.5\text{V}$, 1.0V, and 1.5V, respectively.

Thanks to a comment by one of the referees, we also notice that, in the first part of the discussion in [17], the perturbation (3.3) involves T rather than T_0. The resulting first derivative part of the perturbed system is somewhat more complicated, but with the help of MATHE-MATICA, we are able to determine explicitly its three eigenvalues as

$$\lambda_1 = u, \qquad \lambda_{2,3} = \left[1 + \frac{1}{2}(\gamma - 1)b\right] u \pm \sqrt{[\gamma + b(\gamma - 1)]\frac{p}{mn} + \frac{1}{4}b^2(\gamma - 1)^2 u^2},$$

where $\gamma = \frac{5}{3}$ and the perturbation constant $b = -0.7$, by use of the suggested value $r = 0.72$ of [17]. Clearly, all three eigenvalues are real as long as $n > 0$ and $T > 0$, thus the perturbed system has a hyperbolic first derivative part. This analysis justifies the statement that the perturbation to the HD model proposed in [17] is indeed small mathematically, and the usage of hyperbolic based algorithms is adequate.

The last model we wish to check is the ET model [2]. In this case, the left-hand-side of

(1.2) is defined by

$$w = \begin{pmatrix} emn \\ nE \end{pmatrix}, \qquad f(w) = \phi_x mn \begin{pmatrix} e\mu(E) \\ \mu^E(E) + D(E) \end{pmatrix}, \qquad g(w) = \phi_y mn \begin{pmatrix} e\mu(E) \\ \mu^E(E) + D(E) \end{pmatrix},$$

(3.4)

where n is the concentration, E is the *particle* energy, and ϕ is the electrical potential. The energy E is related to the temperature T in this model by the formula,

$$E = \frac{3}{2}kT\left(1 + \frac{5}{4}\{kT\}\right),$$

(3.5)

and the three (mobility and diffusion) functions of E are defined by

$$\mu(E) = \mu_0 \frac{T_0}{T}, \qquad \mu^E(E) = \frac{3}{2}\mu_0 kT_0\left(1 - \frac{5}{4}\left\{\frac{kT}{e}\right\}\right), \qquad D(E) = k\mu_0 T_0.$$

(3.6)

Here, we have employed a bracket notation to indicate the numerical, as distinct from dimensional, values of $kT, kT/e$. The exact values of the constants can be found in [8]. It is not difficult to obtain a necessary and sufficient condition for $\xi_1 f'(w) + \xi_2 g'(w)$ (for real ξ_1 and ξ_2) to have only real and distinct eigenvalues:

$$\left(\mu(E) - E\frac{d}{dE}\mu(E) - m\frac{d}{dE}\mu^E(E)\right)^2 + 4m\frac{d}{dE}\mu(E)\left(\mu^E(E) + D(E) - E\frac{d}{dE}\mu^E(E)\right) > 0.$$

(3.7)

By substitution of (3.6) into (3.7), after some manipulations, we can verify that inequality (3.7) is valid for any $T > 0$. This proves the hyperbolicity of the first derivative part of the ET model. It also justifies the usage of hyperbolic based ENO schemes in [8].

4 Concluding Remarks

We have assessed the validity of the inertial approximation, by which the hydrodynamic model is reduced by the elimination of certain convective terms. A principal motivation for this approximation is the desire to retain the traditional exponential fitting (Scharfetter-Gummel) numerical methods, which have proven so successful in simulation of the drift-diffusion model.

Our conclusion is that this approximation is not warranted! In particular, it is invalid in the vicinity of junctions of one dimensional devices, and near the contacts of two dimensional devices. However, the full hydrodynamic model possesses hyperbolic modes, which allow for the creation of steep fronts, and even shock formation. This suggests the use of numerical methods explicitly designed for such behavior. We have employed one such method, ENO, and verified its effectiveness.

We have also analyzed the first derivative perturbation of the Fourier law of heat conduction, employed in the model of [17], and determined this to be benign with respect to the hyperbolic character of the HD model. This justifies and suggests the use of shock capturing methods for this model as well. Finally, we have analyzed the appropriateness of such methods for the ET model (termed the RT model in an early version), and found that the first derivative part of this system is hyperbolic as well.

The analysis of the first derivative component of the HD and ET models should not be confused with the mathematical classification of the complete systems. Exclusive of the Poisson equation, these are classified as hyperbolic/parabolic and parabolic, respectively. It is the hyperbolic modes in the HD model which cause numerical fitting difficulty, and, while these components are not technically present in the ET model, due to the second derivative terms, we have found that these terms can be effectively viewed as perturbations from a first order hyperbolic system. It is this viewpoint which distinguishes our analysis from that of Gardner in [4] and [5], where a Fourier mode analysis was employed to examine the full system. This is, of course, equivalent to mathematical classification. Our approach is ultimately motivated by the effectiveness of numerical computation based on hyperbolic methods.

Finally, we should like to mention that, since Scharfetter-Gummel type schemes currently are predominantly used in device simulation, it is important to perform a comprehensive comparison between ENO (or any high resolution hyperbolic based scheme) and Scharfetter-Gummel type

schemes. However, this is beyond the scope of this paper. Such a comparison actually exists in the computational fluid dynamics community, where exponential type methods (the methods similar to Scharfetter-Gummel type methods in device simulation) have been compared with modern high resolution schemes (see, e.g., [10]) and have been shown to be less effective and less accurate for high gradient or shocked solutions. We believe that a high resolution scheme such as ENO has genuine potential in device simulation, based on its success in computational fluid dynamics and the similarity (in mathematical classification) of the equations there, as compared to those of device simulation. What we accomplish in this paper is to establish this link by working out the mathematical classification of the first derivative part for several device simulation models.

References

[1] G. Baccarani and M.R. Wordeman. An investigation of steady-state velocity overshoot effects in Si and GaAs devices. *Solid State Electr.*, 28:407–416, 1985.

[2] D. Chen, E. Kan, U. Ravaioli, C.-W. Shu, and R. Dutton. An improved energy transport model including non-parabolic and non-Maxwellian distribution effects", *IEEE Elec. Dev. Lett.*, 13(1):26–28, 1992.

[3] E. Fatemi, J.W. Jerome, and S. Osher. Solution of the hydrodynamic device model using high-order nonoscillatory shock capturing algorithms. *IEEE Trans. Computer-Aided Design of Integrated Circuits and Systems*, CAD-10:232–244, 1991.

[4] C.L. Gardner. Numerical simulation of a steady state electron shock wave in a submicrometer semiconductor device. *IEEE Trans. Electron Devices*, ED-38:392–398, 1991.

[5] C.L. Gardner. The quantum hydrodynamic model for semiconductor devices. *SIAM J. Appl. Math.*, 54:409–427, 1994.

[6] C.L. Gardner, J.W. Jerome, and D.J. Rose. Numerical methods for the hydrodynamic device model: Subsonic flow. *IEEE Trans. Computer-Aided Design of Integrated Circuits and Systems*, CAD-8:501–507, 1989.

[7] A. Gnudi, F. Odeh and M. Rudan. Investigation of non-local transport phenomena in small semiconductor devices. *European Trans. on Telecommunications and Related Technologies*, 1(3):307–312 (77–82), 1990.

[8] J. W. Jerome and C.-W. Shu. Energy models for one-carrier transport in semiconductor devices. In W. Coughran, J. Cole, P. Lloyd, and J. White, editors, *IMA Volumes in Mathematics and its Applications 59*, pages 185–207. Springer-Verlag, 1994.

[9] J. W. Jerome and C.-W. Shu. The response of the hydrodynamic model to heat conduction, mobility, and relaxation expressions. *VLSI Design*, to appear.

[10] B. P. Leonard. The embarrassing problem of advective modelling. In W. Vogt and M. Mickle, editors, *Modeling and Simulation 23, Part 5.* University of Pittsburgh. pages 2715-2726, 1992.

[11] B. Meinerzhagen, R. Thoma, H.J. Peifer, and W.L. Engel. On the consistency of the hydrodynamic and the Monte Carlo models. In *Proceedings of the Second International Workshop on Semiconductors*, pages 7–12. Beckman Institute, University of Illinois, 1992.

[12] S.C. Lee and T.W. Tang. Transport coefficients for a silicon hydrodynamic model extracted from inhomogeneous Monte-Carlo calculations. *Solid State Electr.*, 35:561–569, 1992.

[13] M. Rudan and F. Odeh. Multi-dimensional discretization scheme for the hydrodynamic model of semiconductor devices. *COMPEL*, 5:149–183, 1986.

[14] Siegfried Selberherr. *Analysis and Simulation of Semiconductor Devices.* Springer-Verlag, New York, 1984.

[15] C.-W. Shu. A numerical method for systems of conservation laws of mixed type admitting hyperbolic flux splitting. *J. Comp. Phys.*, 100:424–429, 1992.

[16] C.-W. Shu and S.J. Osher. Efficient implementation of essentially non-oscillatory shock capturing schemes, II. *J. Comp. Phys.*, 83:32–78, 1989.

[17] M.A. Stettler, M.A. Alam, and M.S. Lundstrom. A critical examination of the assumptions underlying macroscopic transport equations for silicon devices. *IEEE Trans. Electron Devices*, 40:733–740, 1993.